Design of Adhesive Anchors For Seismic Regions
Static Tension Tests

Eric E. Matsumoto, Ph.D., P.E
California State University, Sacramento, Sacramento, CA

Bartt R Gunter, P.E
California Department of Transportation, Sacramento, CA

ABSTRACT
Recent Caltrans applications of drill-and-bond anchors require a design method that ensures a ductile failure under seismic conditions. In addition, a more flexible and transparent design method is sought for a wide range of reinforcing bar sizes. As the first step in addressing these needs, an experimental research program is being conducted to establish a general design methodology to calculate the seismic tensile capacity of a single drill-and-bond rebar anchored in uncracked concrete using Set-45 as the adhesive. Forty-six static tension tests of a drill-and-bond rebar (#5 to #11) anchored in uncracked concrete using Set-45 have been conducted. Specimens failed in one of three modes: bond, splitting or bar fracture. Static test results to date have indicated that a ductile failure can be ensured by designing the fracture load to be the lowest failure load. Conclusions based on both static and tension cyclic test results will be reported by February 2006. Future sponsored research is expected to address additional variables such as threaded bars, epoxy-coated bars, additional adhesive products, edge effects, group effects, shear, combined tension and shear, and cracked concrete. This will allow the design methodology to be expanded to a wide range of drill-and-bond applications.

INTRODUCTION
Due to the rapid population growth throughout the U.S., many applications exist where designers need to fasten new structures to hardened concrete to maintain or expand the existing infrastructure. Typical examples of such applications are barrier rail replacement, bridge widening, and seismic retrofit. This is commonly achieved through anchors installed into existing concrete, known as post-installed anchors.

Various post-installed anchorage systems have been developed and are typically classified as either mechanical or bonded anchors. Mechanical anchors can be subdivided into undercut and expansion anchors while bonded anchors can be subdivided into adhesive and grouted anchors. Adhesive anchors are often defined as anchors having hole diameters less than approximately 1.5 times the bar diameter, whereas grouted anchors typically have a larger hole diameter at least 1.5 times the bar diameter. A variety of products are used for bonding or grouting the anchors. For

all systems, the means of load transfer is by bearing, mechanical interlock, bond, friction, or a combination of these mechanisms. (1,2)

Problem Statement

Section 5 of the California Department of Transportation's (Caltrans) Bridge Design Aids Manual (BDA) addresses four of the most widely used anchorage systems available to the designer. For anchoring into existing concrete, one simple and economical method that uses grouted or bonded steel anchors has been "strongly recommended whenever applicable." (3) The construction procedure consists of drilling holes to a specified depth and diameter, preparing the holes, filling holes with a bonding material, and then placing either reinforcing steel bars (rebars) or threaded rods into each hole. This approach is appropriately known as "Drill-and-Bond Dowel" for an anchor bonded with magnesium phosphate concrete or "Drill-and-Grout Dowel" for an anchor bonded with cementitious grout.

Caltrans recognizes that the guidelines in the BDA for the design of post-installed anchors are fairly restrictive. (4) As shown in Table 1, the BDA provides a table with recommended tension and shear design strength values for rebar sizes #5 through #8.

TABLE 1 Caltrans Bridge Design Aids for Post-Installed Anchors (3)

Design Data for Grade 60 Deformed Bar Reinforcement								
Size of Rebar	Minimum Edge Distance	Minimum Embedment Depth	Hole Diameter		Design Strength (kips)			
					Grout		Bond	
			Grout	Bond	Tension	Shear	Tension	Shear
#5	3"	5"	7/8"	1 1/8"	3.1	8.2	10.5	8.2
#6	4"	6"	1"	1 1/4"	4.4	11.6	14.8	11.6
#7	4"	7"	1 1/8"	1 3/8"	6.0	15.8	20.3	15.8
#8	5"	8"	1 1/4"	1 1/2"	7.9	20.8	26.7	20.8

The table denotes a specific drilled hole diameter, minimum embedment depth, and minimum required edge distance for each anchor size. Different design strengths are given for anchors, depending on the bonding material: cementitious grout (drill-and-grout) or magnesium phosphate concrete (drill-and-bond).

It is important to note that the embedment depths specified in the BDA tables may not be sufficiently large to develop a ductile failure characterized by yielding and fracture of the steel anchor. The only guideline that the BDA contains for an application requiring a ductile system is the following unsupported statement: "Generally, holes having two times the minimum embedment depth for reinforcement bars or 1.5 times the minimum embedment depth for threaded rods will develop the ultimate strength of the embedment steel."

Many applications exist where engineers use the tables in the BDA for anchors with parameters that extend beyond the range of the existing guidelines. Examples of this include connections subjected to forces larger than those permitted by the BDA or connections with edge distances

less than the minimum due to geometric constraints. Thus, there exists the need to develop a flexible design methodology with the capability of designing anchors beyond the BDA limits. With the development of a new design methodology, realistic design strengths for anchors embedded to depths greater than those shown in Table 1 may be obtained. In addition, the embedment depth required to achieve a ductile failure associated with full development of the anchor may be determined.

RESEARCH OBJECTIVE AND APPROACH

The primary objective of the first phase of research is to establish a general design methodology to calculate the seismic tensile capacity of a single drill-and-bond rebar (#5 to #11) anchored in uncracked concrete using Set-45. Results will provide a solid basis for subsequent research to expand the design methodology to address additional variables including threaded bars, epoxy-coated bars, additional adhesive products, edge effects, group effects, shear, combined tension and shear, and cracked concrete.

Table 2 shows the test matrix and results for select data. Select data is tabulated because some test results were adversely affected by carbonation and poor mixing and are not addressed in this paper. As shown in the table, a limited number of variables are investigated, including #5, #8, and #11 uncoated rebars bonded with magnesium phosphate concrete. For each anchor size, two embedment depths were tested: 1) a shallow embedment (~$8d_b$) such that a brittle failure occurred prior to bar fracture; and 2) a deep embedment (~$14–16d_b$) such that a ductile steel failure occurs, characterized by bar yield and fracture. The shallow embedment tests exhibit a brittle failure mode, allowing the tensile capacity to be determined for calibration of the design equation. The deep embedment tests provide evidence that anchors are fully developed to fracture. Both are important objectives. Tests were generally conducted in accordance with ICBO Acceptance Criteria 58. (5) Figure 1 shows a typical test setup for static tests.

FIGURE 1 Static Test Setup

SUMMARY OF TEST RESULTS

This paper summarizes static tension test results. Cyclic tests are still underway. As shown in Table 2, shallow embedment tests generally produced a bond or splitting failure, often after bar yield, whereas deep embedment tests produced bar fracture, as intended in the specimen design. At larger loads, a shift in failure mode from bond failure to a splitting failure was observed,

despite the use of specimens and bearing rings with edge distances exceeding that required by ASTM E488. (6) For all specimens, an appropriately stiff load-deflection response was achieved. Figure 2 shows representative failure modes from the static tests.

TABLE 2 Select Static Test Data

Test ID	d_b (in)	h_{ef}[A] (in)	h_{ef}/d_b	f'_{cg} (psi)	Failure Mode[B]	P_{max} (kips)	P_{max}/P_y[C]	Slip[D] (in)
S5-8A	0.625	5.00	8.00	5950	B	19.2	0.96	-[F]
S5-8E	0.625	5.00	8.00	7333	Y/B	24.1	1.18	0.015
S5-8F	0.625	5.00	8.00	8467	Y/B	22.0	1.08	0.034
S5-8G	0.625	5.00	8.00	7333	Y/B	21.1	1.03	0.018
S5-8H	0.625	5.00	8.00	5950	Y/B	22.7	1.22	-[F]
S5-8I	0.625	5.00	8.00	6258	B	18.0	0.90	0.025
S5-8J	0.625	5.00	8.00	6900	F	27.0	1.33	0.015
S5-8K	0.625	5.00	8.00	6900	F	25.7	1.31	0.015
S5-8L	0.625	5.00	8.00	6258	F	25.4	1.26	0.019
S5-8M	0.625	5.00	8.00	6625	F	24.3	1.30	0.030
S5-8N	0.625	5.00	8.00	6600	F	24.6	1.29	0.009
S5-16A	0.625	10.00	16.00	6500	F	21.0	1.01	0.023
S5-16B	0.625	10.00	16.00	6021	F	25.3	1.30	0.022
S5-16C	0.625	10.00	16.00	6021	F	25.1	1.29	0.011
S5-16D	0.625	10.00	16.00	5950	F	24.7	1.27	0.002
S5-16E	0.625	10.00	16.00	5950	F	27.0	1.35	0.035
S8-8H	1.000	8.00	8.00	6908	Y/S	59.8	1.16	0.005
S8-8I	1.000	8.00	8.00	6908	Y/S	53.0	1.01	0.018
S8-8J	1.000	8.00	8.00	7058	Y/S	58.2	1.09	0.006
S8-8K	1.000	8.00	8.00	7521	Y/S	53.9	1.03	0.052
S8-8L	1.000	8.00	8.00	7521	S	39.6	0.76	0.012
S8-16A	1.000	16.00	16.00	6900	F	69.4	1.30	0.017
S8-16B	1.000	16.00	16.00	6900	F	69.3	1.37	0.040
S11-8F	1.410	11.00	7.80	6600	S	73.8	0.70	0.042
S11-8G	1.410	11.25	7.98	7217	S	83.1	0.78	0.031
S11-8I	1.410	11.25	7.98	6900	S	75.7	0.71	0.015
S11-8J	1.410	11.25	7.98	7217	S	74.9	0.71	0.012
S11-14A[E]	1.410	19.74	14.00	7367	Y/S	139.6	1.32	0.011
S11-14B[E]	1.410	19.74	14.00	7625	Y/S	143.3	1.35	0.012

NOTES:

A. h_{ef} represents actual embedment depth, measured post-test for failures other than bar fracture.
B. B=Bond failure; Y/B=Bar yield followed by bond failure; F=Bar fracture; S=Splitting failure; Y/S=Bar yield followed by splitting failure; BC=Bond failure through pre-existing crack.
C. P_y refers to yield force of bar, accounting for intentional reduction in bar area below LVDT bracket (to control failure location). Applies only to cases in which yield occurred.
D. Slip represents bar slip at top surface of specimen relative to top surface. For bond failures prior to bar yield, slip is taken as the slip at maximum load, P_{max}. For cases in which bar yielded, slip refers to slip at bar yield.
E. Onset of bar fracture, but characterized by Y/S. Maximum load exceeded expected fracture load.
F. No data available.

A. Bond **B. Splitting** **C. Bar Fracture**

FIGURE 2 Failure Modes for Static Tests

General Observations

Bond failures exhibited a different mechanism than splitting failures. However, as shown in Figure 3, both failure modes produce capacities that are proportional to embedment depth. This trend holds even when the load is normalized to account for variation in concrete and adhesive strengths. For bond failures, this linear trend is expected, as the bond strength depends on the bonded area, which is proportional to the embedment depth, h_{ef}, assuming the approximation of a uniform bond strength along the bar embedment.

A splitting failure occurs when the circumferential tensile splitting stresses produced by the bearing of concrete on the inclined lugs of a rebar exceed the tensile capacity of the concrete. This implies that the splitting failure load in the splitting plane, $P_{split\text{-}plane}$, is dependent on the area of the splitting failure plane and the tensile strength of the concrete, as shown below:

$$P_{split\text{-}plane} = (\textit{Splitting Tensile Strength of Concrete})(\textit{Area of Splitting Plane})$$

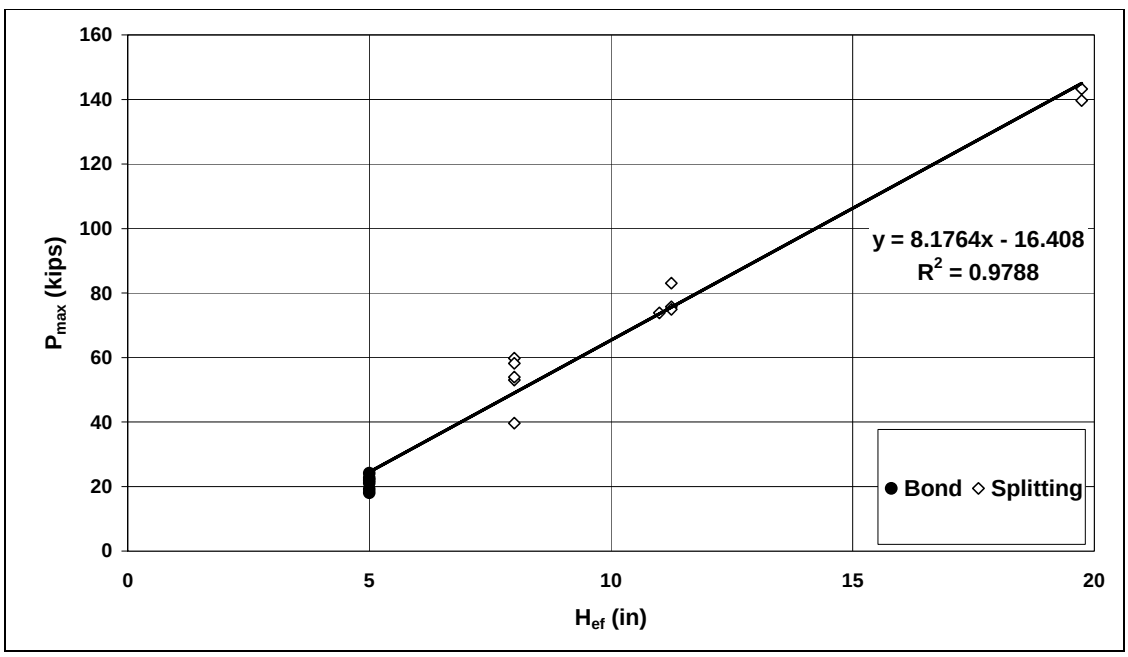

FIGURE 3 Maximum Applied Load vs. Embedment Depth (Select Static Test Data)

Various researchers have shown that other factors must also be considered to accurately determine the splitting strength of concrete for development of reinforcing bars or splices. For example, Canbay and Frosch (7) have demonstrated the importance of the c/d_b ratio in determining an effective cover, c_{eff}, for the splitting plane in calculating $P_{split\text{-}plane}$:

$$P_{split-plane} = 2(6\sqrt{f_c'})(c_{eff} \times h_{ef}) \quad (1)$$

For a splitting failure, the tensile capacity of the bar, P_{split}, in the longitudinal direction (i.e., in the vertical direction for static pullout tests) can be determined from the relationship between $P_{split\text{-}plane}$ and P_{split} using the angle β as shown below:

$$\tan\beta = P_{split\text{-}plane} / P_{split}$$

Solving for P_{split} and substituting $P_{split\text{-}plane}$ from (1) leads to:

$$\text{Splitting: } P_{split} = P_{split-plane} / \tan\beta = 6\sqrt{f_c'}(2c_{eff} \times h_{ef})\cot\beta \quad (2)$$

The term ($2c_{ef} \times h_{ef}$) applies only for a bar with symmetric cover but can be modified for different splitting plane areas.

Because the circumferential tensile stresses drop off rapidly at increasing distances from the bar, an effective cover of only several inches is typically effective (i.e., subject to a uniform tensile stress), regardless of an actual larger cover. Radial splitting cracks that formed in the static test specimens generally extended to the embedment depth of the bar. Therefore, the splitting plane and thus splitting capacity of the bar should be approximately proportional to the embedment depth, h_{ef}.

Bond Strength Results

Based on a uniform bond strength model, bond failure produced an average bond strength of ~2300 psi, which is within the range of values from the adhesive anchor tests of Reference 1. A reasonably low coefficient of variation of 0.13 for the select bond strength failures of Table 2 was observed.

For cases in which bond failure governs, the bond strength value can be used to estimate the capacity of a single bar loaded statically in tension, without edge or group effects, as follows:

$$\text{Bond: } P_{bond} = 2.3\pi d_b h_{ef} \ (kips) \quad (3)$$

Splitting Strength Results

Figure 4 plots the maximum applied load, P_{max} versus the area of splitting plane, A_{split}. A linear trend is evident by the r^2 term of 0.93. The linearity confirms that the area of the splitting plane is the main factor affecting splitting capacity. A similar analysis using the maximum load normalized by the square root of the compressive strength ($P_{max}/f'c^{0.5}$) indicated little effect due to concrete strength. This is expected because of the fairly narrow range of concrete strengths that were achieved on test day (~4400-5100 psi).

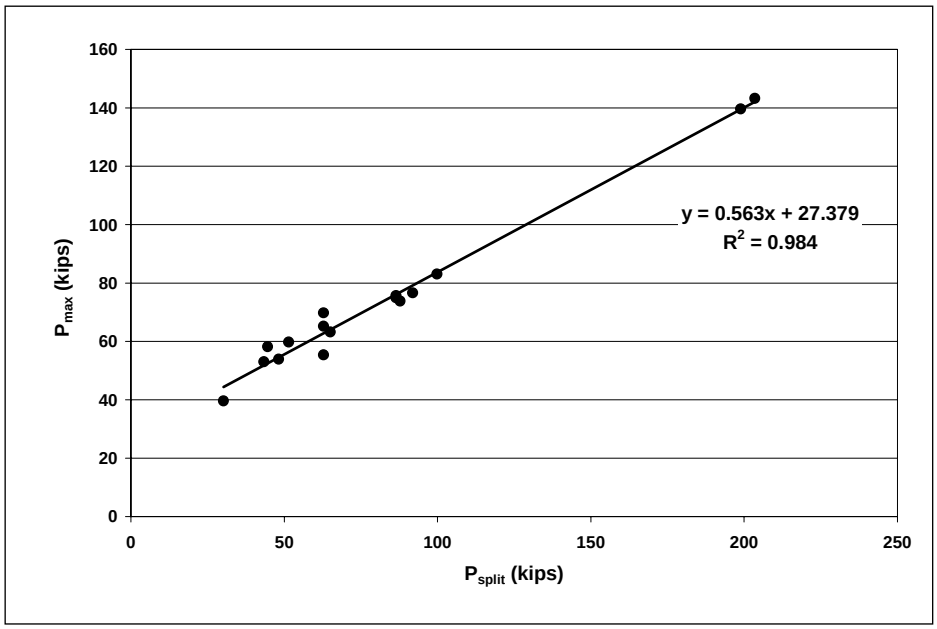

FIGURE 4 Maximum Applied Load vs. Area of Splitting Plane

Figure 5 plots P_{max} vs. P_{split} for the case of β equal to 22 degrees. A reasonable linearity and coefficient of variation demonstrate that the prediction approach is reliable. However, a reduction in coefficient of variation resulted when β was varied to be 18 degrees for #8 bars and 25 degrees for #11 bars. Design using a single value for β may provide an accurate enough approach for determining the splitting capacity. Edge distance and bar spacing are important parameters in establishing the splitting capacity.

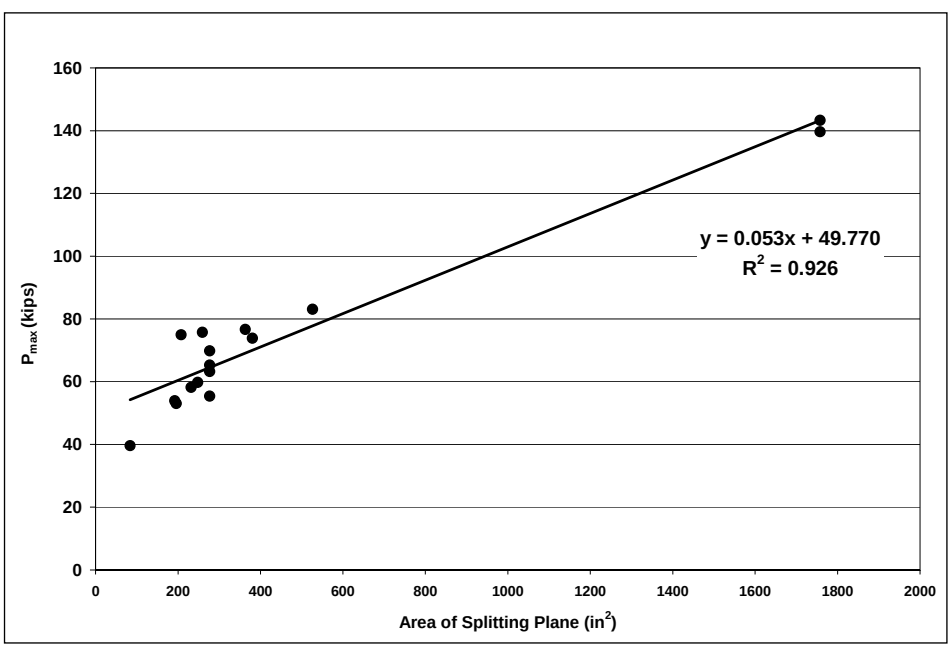

FIGURE 5 Maximum Applied Load vs. Splitting Capacity (Beta=22 degrees)

Bar Fracture Results

Because the test bars were slightly reduced in cross section to control the failure location, fracture loads were typically reduced several percent. However, as shown in Table 2, the consistently reliable anchorage behavior at an embedment depth of $16d_b$ indicates that, under static conditions, a ductile design assuming anchorage to fracture can be reliably designed for at an embedment depth of 16 bar diameters for all bars in the range of #5's to #11's. Test results also indicate that bar fracture may be feasible at a smaller embedment depth, especially for smaller diameter bars such as #5's.

It should be noted that these results apply to a single bar subjected to monotonic tension.

$$\text{Bar Fracture: } P_{fracture} = A_s f_{ute} \qquad (4)$$

SUMMARY AND CONCLUSIONS

Static tests produced bond, splitting, or bar fracture failure modes. Failure loads can be reasonably predicted using Equations (2), (3), and (4). The static capacity for a single bar in tension may be taken as the minimum of the three failure loads, as follows:

$$P_{\max} = \min(P_{bond}, P_{split}, P_{fracture})$$

A ductile failure may be designed by ensuring $P_{fracture}$ is the smallest of these three failure loads. Appropriate load factors and strength reduction factors are necessary to provide an adequate safety margin in design.

It is anticipated that, based upon results of static tests and on-going tension cyclic tests, a general design methodology will be developed to calculate the seismic tensile capacity of a single drill-and-bond rebar (#5 to #11) anchored in uncracked concrete using Set-45. Results will thus provide a new basis for design of drill and bond anchors. Future sponsored research addressing additional variables will allow the design methodology to be expanded to a wide range of applications.

ACKNOWLEDGEMENT

This research was sponsored by the Office of Earthquake Engineering, California Department of Transportation, Contract #59A0424. The assistance of the Caltrans Research Team, including Dr. Saad El-Azazy, Issam Nourredine, Dr. Allaoua Kartoum, and Bob Meline, is gratefully acknowledged. The support of the CSUS student research assistants and laboratory technicians is also gratefully acknowledged.

KEYWORDS

adhesive anchor, pullout, bond, splitting

NOTATION

f_c' = concrete compressive strength, psi

h_{ef} = embedment depth, in

c = concrete cover, in

d_b = bar diameter, in

c_{eff} = effective cover= $0.77c\sqrt{c/d_b}$, in

A_s = area of reinforcing bar, in^2

f_{ute} = expected ultimate tensile strength of rebar (fracture), ksi

REFERENCES

1. Cook, R. A.; Kunz, J.; Fuchs, W.; and Konz, R.; "Behavior and Design of Single Adhesive Anchors under Tensile Load in Uncracked Concrete," *ACI Structural Journal*, V. 95, No. 1, January-February 1998, pp. 9-26.
2. Zamora, N. A.; Cook, R. A.; Konz, R. C.; and Consolazio, G. R., "Behavior and Design of Single, Headed and Unheaded, Grouted Anchors under Tensile Load," *ACI Structural Journal*, V. 100, No. 2, February-March, 2003, pp. 222-230.
3. California Department of Transportation, Bridge Design Aids Manual, State of California Department of Transportation Publication Distribution Unit, California, March 1991, Section 5, pp. 5-81 – 5-88.
4. California Department of Transportation, Research Problem Statement, "Drill and Bond to Develop the Full Capacity of Rebar/Development Length," Office of Earthquake Engineering and Design Support, 2003.
5. "Acceptance Criteria for Adhesive Anchors in Concrete and Masonry Elements," Acceptance Criteria 58, International Conference of Building Officials, Evaluation Services, Inc., December 2001.
6. ASTM, 1996, Standard Test Methods for Strength of Anchors in Concrete and Masonry Elements (ASTM E488-96)," 2002 Book of ASTM Standards, V. 04.11, West Conshohockem, PA, pp. 65-72.
7. Canbay, E., Frosch, R. J., "Bond Strength of Lap-Spliced Bars," ACI Structural Journal, Accepted for Publication, 2005.